

Scaling Rules for Isocratic Elution Chromatography

Scaling rules for both linear and nonlinear elution chromatography with independent solutes are discussed. The scaling method utilizes smaller diameter particles with high mass transfer rates. The column length, diameter, and cycle time are then scaled so that pressure drop, separation, and throughput are the same or better than in the old design. The new design uses much less packing and cycles more rapidly than the old design. Mathematical derivation shows that the scaling rules for systems with linear and nonlinear isotherms are the same in certain circumstances. Gaussian solutions are used for studying linear systems. Mass transfer zone and diffusive wave analyses are used for constant and proportional patterns, respectively, to describe elution when plateaus form at the feed concentration. Numerical examination of the constant-pattern elution curve using the Thomas solution shows that the scaling rules are applicable to short columns, which means that there is a negligible entrance effect on the scaling rules. The Thomas solution also shows that the mass transfer resistance has little effect on the scaling rules for the proportional-pattern wave of a nonlinear solute. Shock and diffusive wave analyses based on the local equilibrium model are employed to describe the separation when the elution curves do not have plateaus. The calculated results show that the scaling rules are followed exactly when pore diffusion controls. Separation of two noninteracting nonlinear components and of a linear and a nonlinear component remains constant when these scaling rules are followed. Several example calculations are used to demonstrate the method.

Phillip C. Wankat, Yoon-Mo Koo

School of Chemical Engineering
Purdue University
West Lafayette, IN 47907

Introduction

Preparative and large-scale chromatographic systems have been the subject of considerable research and commercial activity recently (Bidlemyer, 1987; Guiochon and Colin, 1986; Knox and Pyper, 1986; Ladisch et al., 1984; Pieri et al., 1983; Verzele and Dewaele, 1985; Wankat, 1986a,b). This area includes columns from about 2 cm to 4 m diameter. Reported commercial separations have varied from very high value, low-volume pharmaceuticals to low-value, high-volume sugars. A variety of operating methods, column geometries, packing sizes, and packing procedures have been reported. Large-scale and preparative chromatography are clearly very exciting areas that are rapidly changing.

The purposes of this paper are to theoretically explore the effects of particle diameter and to develop scaling methods for large-scale isocratic elution chromatography (these terms are defined later). This exploration will also force us to consider column geometry and cycle time. Later papers will consider nonlinear nonisocratic systems and compressible packings.

The question of particle size in preparative and large-scale chromatographic systems has been explored previously. Unfortunately, there is not agreement on what particle size to use. A survey of readers using preparative systems (up to about 1 in. [25 mm] dia.) reported that 10 to 15 μm spherical particles were most popular (Majors, 1985). The use of 10 μm particles has been strongly suggested for preparative columns (Guiochon and Colin, 1986; Verzele and Dewaele, 1985). In larger scale systems larger particles, such as 20 to 40 mesh, have been used (Pieri et al., 1983; Verzele and Dewaele, 1985; Ladisch et al.,

The present address of Y.-M. Koo is Inha University, Incheon, South Korea.

1984). The usual rationale for going to larger diameter particles is that pressure drop becomes excessive with small particles and much of the efficiency advantage is lost because of column overloading. However, if the column is scaled properly small particles can be used without increasing the pressure drop (Wankat, 1986a,b). The previous theoretical analysis (Wankat, 1986a,b) was restricted to cases where pore diffusion controlled the mass transfer and both pressure drop and the separation were kept constant. In this paper the analysis will be extended to a variety of other cases for isocratic systems.

Our approach will be to assume that an existing design is satisfactory for the large-scale chromatographic separation. This existing design may have been developed either experimentally or theoretically. We will then explore the effects of scaling several variables in an attempt to improve the design. This approach is an extension of the chromatographic results reported earlier (Wankat, 1986a,b) and is similar to the analysis of adsorption and ion exchange systems (Wankat, 1987). Snyder (1972) used a similar method except that particle diameter d_p was held constant. The scaling factors are

$$a = \frac{d_{p,new}}{d_{p,old}}, b = \frac{L_{new}}{L_{old}}, c = \frac{D_{new}}{D_{old}}, R_p = \frac{\Delta p_{new}}{\Delta p_{old}}, R_q = \frac{Q_{new}}{Q_{old}} \quad (1)$$

The parameter R_q is useful for scaling-up from bench or pilot to commercial scale.

Review of Linear Chromatography

Chromatography is often operated with all solutes migrating through the column with finite velocities. If the solvent composition is kept constant, the operation is called isocratic. Operation where a pulse of feed is followed by a less strongly adsorbed solvent is called elution chromatography. Operation where a pulse of feed is preceded by a less strongly adsorbed solvent and followed by a more strongly adsorbed solvent is called displacement chromatography, which will be the subject of a later paper. Migration is the most common analytical method and is used in some large-scale systems. In this paper methods for scaling chromatography by changing the particle diameter will be developed for migration chromatography with linear isotherms, using familiar chromatography concepts. The packing is assumed to be rigid. We will assume that a good solvent system with adequate values of relative retention and selectivity has been developed. The packing is assumed to have an infinite life and operation is with repeated feed pulses.

The pressure drop in a packed bed of rigid particles in laminar flow is (Bird et al., 1960)

$$\Delta p = \frac{\mu v_0 L}{K d_p^2} \quad (2)$$

where K is the permeability, which is related to the porosity in a packed bed.

$$K = \frac{\epsilon^3}{150(1 - \epsilon)^2} \quad (3)$$

Obviously, Δp will increase as d_p decreases unless v and/or L are changed. The superficial fluid velocity in the column can be

determined as

$$v_0 = \frac{4Q}{\pi D^2} \quad (4)$$

where Q is the volumetric flow rate.

For linear systems the separation can be determined in terms of the number of stages N

$$N = L/H \quad (5)$$

where H is the height equivalent to an equilibrium stage. For short feed pulses and long columns the resulting linear solution is Gaussian.

$$c_i = c_{max,i} \exp \left[- (t - t_{R,i})^2 / 2 \left(\frac{LH}{u_i^2} \right) \right] \quad (6)$$

where u_i is the solute velocity and $t_{R,i}$ is the retention time. The solute velocity is

$$u_i = \frac{v}{1 + k'_i} = \frac{v}{1 + \frac{1 - \epsilon}{\epsilon} \rho_B K_i} = \frac{v_0}{\epsilon + (1 - \epsilon) \rho_B K_i} \quad (7)$$

where k'_i is the capacity factor and K_i is the linear equilibrium constant. The retention time is the time when the peak maximum exits. This is

$$t_{R,i} = L/u_i \quad (8)$$

The Gaussian solution is exact for infinitesimal feed pulses. The exact solution for finite feed pulses can be obtained by superposition of the solution for a step input with the solution for a step decrease in feed concentration (Lightfoot et al., 1962). The resulting solution contains error functions. This solution can often be closely approximated by the Gaussian solution if the retention time of the peak is determined from the center of the feed pulse. Use of these solutions is expected to agree with the scaling results obtained with the Gaussian solution.

For linear systems with short feed pulses the separation is usually defined in terms of the resolution R . The resolution is defined as

$$R = \frac{2(t_{R2} - t_{R1})}{w_1 + w_2} \quad (9)$$

where the peak width in time units is four times the standard deviation measured in time units.

$$w_i = 4\sigma_{t,i} = \frac{(LH_i)^{1/2}}{u_i} \quad (10)$$

In these equations species 2 is the more strongly adsorbed species, which thus exits from the column later.

Substituting Eqs. 8 and 10 into Eq. 9 gives

$$R = \frac{L^{1/2} \left(\frac{1}{u_2} - \frac{1}{u_1} \right)}{2 \left(\frac{H_2^{1/2}}{u_2} + \frac{H_1^{1/2}}{u_1} \right)} \quad (11)$$

which becomes

$$R = \frac{L^{1/2}}{2} \frac{k'_2 - k'_1}{(1 + k'_2)H_2^{1/2} + (1 + k'_1)H_1^{1/2}} \quad (12)$$

after substituting in Eq. 7. In chromatography we often separate molecules that are very similar. Thus the relative retentions are close and $H_1 = H_2$. In this case Eq. 12 can be simplified to

$$R = \frac{1}{2} \left(\frac{\alpha - 1}{1 + \alpha} \right) \frac{\bar{k}'}{1 + \bar{k}'} N^{1/2} \quad (13)$$

where \bar{k}' is the arithmetic average capacity factor and α is the selectivity.

$$\bar{k}' = \frac{k'_1 + k'_2}{2}, \quad \alpha = \frac{k'_2}{k'_1} = \frac{K_2}{K_1} \quad (14)$$

Equation 13 is sometimes known as the fundamental equation of linear chromatography.

In order to use this model, we must be able to predict the height equivalent to a theoretical plate (HETP) value, H . By comparing plate theory to a mass transfer analysis, Van Deemter et al. (1956) derived the following expression for H :

$$H = A + \frac{B}{v} + Cv \quad (15)$$

where

$$A = \lambda d_p \quad (16)$$

is the contribution due to eddy dispersion,

$$B = 2\gamma D_M \quad (17)$$

is the contribution due to molecular diffusion, and

$$C = C_M + C_{SM} = \frac{c_M d_p^2}{D_M} + \frac{c_{SM} d_p^2}{D_{SM}} \quad (18)$$

is the mass transfer contribution. In the usual velocity range for large-scale separations the mass transfer, C , terms are dominant. When pore diffusion controls, the number of plates N is proportional to L/vd_p^2 . Scaling rules for this case are particularly simple and were developed previously (Wankat, 1986a,b). A variety of other forms for predicting H have been developed and are reviewed by Grushka et al. (1975).

An empirical equation with the following form

$$H = kv^n d_p^{n+1} \quad (19)$$

will be used later to derive very simple scaling rules. Equation 19 reduces to the Snyder equation (Snyder, 1972; Grushka et al., 1975) for constant d_p and is a special case of the dimensionless form of the Knox equation (Grushka et al., 1975). Equation 19 also agrees with mass transfer correlations. The advantage of a simple form such as Eq. 19 is that the resulting scaling laws will be quite simple. The disadvantage is that the equation is only approximate over wide ranges of v and d_p . If pore diffusion con-

trols, $n = 1$, while if film diffusion controls n is approximately 0.5. We will assume that changes in the particle diameter and the velocity are within the range where n is constant. The number of stages in the column becomes

$$N = \frac{L}{kv^n d_p^{n+1}} \quad (20)$$

General Scaling Method for Linear Systems

The old design is assumed to have a satisfactory pressure drop and resolution. Changes in particle diameter d_p , column diameter D , and length L are assumed to have no effect on porosity ϵ , equilibrium K_i , or selectivity α . The general procedure we will use is to write equations, such as Eq. 2, for both the old and new designs. Taking the ratio of these equations, we obtain scaling equations. Simultaneous solution of these equations will give us the scaling rules.

Pressure drop for the old and new columns can be obtained from Eq. 2. Writing this equation for the new and old designs, and taking the ratio we obtain

$$R_p = \frac{\Delta p_{new}}{\Delta p_{old}} = \frac{bR_q}{a^2c^2} \quad (21)$$

where the scaling factors a , b , c , and R_q were defined in Eq. 1. If $R_p = 1$, then the two columns will have the same pressure drop. If $R_p < 1$, then the new column will have a lower pressure drop.

Equation 12 is the general expression for resolution. Writing this equation for the old and new designs, and taking the ratio we obtain

$$\frac{R_{new}}{R_{old}} = \left(\frac{L_{new}}{L_{old}} \right)^{1/2} \frac{[(1 + k'_2)H_2^{1/2} + (1 + k'_1)H_1^{1/2}]_{old}}{[(1 + k'_2)H_2^{1/2} + (1 + k'_1)H_1^{1/2}]_{new}} \quad (22)$$

In Eq. 22 we have assumed that changing the particle diameter does not change the equilibrium and packing characteristics of the packing. Thus k'_1 and k'_2 are the same in the old and new designs. Equation 22 is quite general since an equation form for H has not been assumed. If the solutes have equal H values, $H_{1,old} = H_{2,old}$ and $H_{1,new} = H_{2,new}$, Eq. 22 simplifies to

$$\frac{R_{new}}{R_{old}} = b^{1/2} \left(\frac{H_{old}}{H_{new}} \right)^{1/2} \quad (23)$$

If the column is scaled to be shorter, the peaks will exit earlier. For feed pulses of finite width, resolution will not remain constant unless the feed pulse is shortened. The same separation will be obtained if the feed period is scaled in the same way as the retention times of the solutes.

$$\frac{(\text{Feed period})_{new}}{(\text{Feed period})_{old}} = \frac{(L/v)_{new}}{(L/v)_{old}} = \frac{(LD^2/Q)_{new}}{(LD^2/Q)_{old}} = bc^2/R_q \quad (24)$$

This scaling keeps the relative movement of the solute waves constant. To have the same throughput of feed with shorter feed pulses the cycle time must be decreased. The resolution of overlapping peaks from adjacent feed pulses will be constant if the old and new designs have the same number of stages and the cycle time is scaled in the same way as the retention times.

$$\frac{(\text{Cycle time})_{\text{new}}}{(\text{Cycle time})_{\text{old}}} = \frac{(L/v)_{\text{new}}}{(L/v)_{\text{old}}} = bc^2/R_q \quad (25)$$

Note that Eqs. 24 and 25 depend in the same way on the scaling parameters.

Simultaneous solution of Eqs. 21 and either Eq. 22 or Eq. 23 requires an expression for H . Simple analytical solutions are developed in the next section. In the remainder of this section we will illustrate a case study approach. This approach is useful when the expression for H is complex or when experimental values of H are available.

Assume that d_p , L , v , R , and Q are known for the old design. The case study approach specifies:

1. A value of $d_{p,\text{new}}$ which specifies $a = d_{p,\text{new}}/d_{p,\text{old}}$
2. A value for $R_q = Q_{\text{new}}/Q_{\text{old}}$
3. A value for $R_p = \Delta p_{\text{new}}/\Delta p_{\text{old}}$

The values for R_q and R_p will often be unity. Since H_1 and H_2 both depend on v , it is convenient to use v as a trial variable. We thus choose a value for v and calculate H_1 and H_2 from the experimental data. The value of $c = D_{\text{new}}/D_{\text{old}}$ can be determined by taking the ratio of Eq. 4 for the old and new designs:

$$c = \frac{D_{\text{new}}}{D_{\text{old}}} = \left[\frac{R_q}{(v_{\text{new}}/v_{\text{old}})} \right]^{1/2} \quad (26)$$

The pressure drop ratio, Eq. 21, can be solved for b :

$$b = \frac{L_{\text{new}}}{L_{\text{old}}} = \frac{R_p a^2 c^2}{R_q} \quad (27)$$

Then the ratio of resolutions can be determined from Eq. 22 or Eq. 23. If $R_{\text{new}}/R_{\text{old}}$ is not the desired value, a new velocity is selected and the procedure is repeated.

The case study approach will be illustrated using the analytical chromatography data of Dong and Gant (1984) for *t*-butyl benzene in 4.6 mm ID columns with 10, 5, and 3 μm dia. C18 bonded phase packings. These data are illustrated in Figure 1. We will assume that *t*-butyl benzene will be separated from a

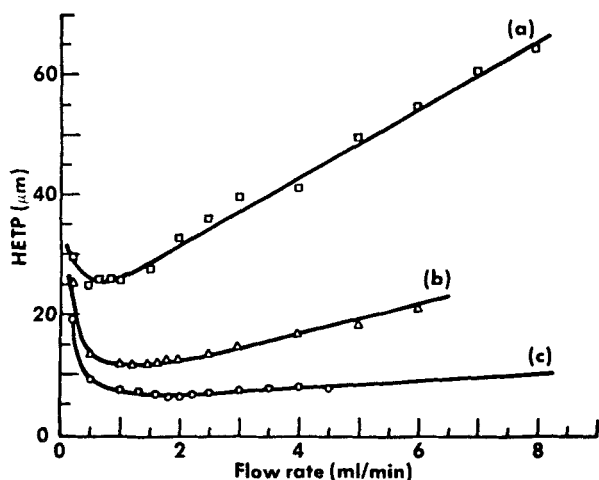


Figure 1. HETP vs. flow rate.

(a) 10 μm particles; (b) 5 μm particles; (c) 3 μm particles
Sample is *t*-butyl-benzene (Dong and Gant, 1984).
Reprinted with permission from *LC, Liq. Chromatogr. HPLC Mag.*, 2(4) (1984), copyright 1984 Aster Publishing Co.

similar compound with the same H value. The old design has: $d_{p,\text{old}} = 10 \mu\text{m}$, $L_{\text{old}} = 25 \text{ cm}$, and $v_{0,\text{old}} = 8/A_c \text{ mL/min}$. From Figure 1 $H_{\text{old}} = 65 \mu\text{m}$. We desire to use a new design with the same pressure drop, $R_p = 1$, the same volumetric flow rate, $R_q = 1$, and the same or better resolution. For the new design we want to use $d_{p,\text{new}} = 5 \mu\text{m}$, which gives $a = 1/2$.

For a first guess assume $v_{\text{new}} = v_{\text{old}}$ (in the next section we will show that this will be valid if Eq. 19 holds with $n = 1$). Then from Figure 1, $H_{\text{new}} = 25 \mu\text{m}$. From Eq. 26, $c = D_{\text{new}}/D_{\text{old}} = 1$. From Eq. 27, $b = L_{\text{new}}/L_{\text{old}} = 1/4$. Then from Eq. 23,

$$\frac{R_{\text{new}}}{R_{\text{old}}} = b^{1/2} \left(\frac{H_{\text{old}}}{H_{\text{new}}} \right)^{1/2} = \left(\frac{1}{4} \right) \left(\frac{65}{25} \right)^{1/2} = 0.806$$

Thus the assumed velocity does not give the desired equal or better resolution.

For the second guess assume $v_0 = 0.75 v_0$. Then from Figure 1, $H_{\text{new}} = 21 \mu\text{m}$. From Eq. 26,

$$c = \left(\frac{1}{3/4} \right)^{1/2} = 1.155$$

from Eq. 27,

$$b = \frac{(1) \left(\frac{1}{2} \right)^2 (1.155)^2}{(1)} = 0.333$$

and from Eq. 23,

$$\frac{R_{\text{new}}}{R_{\text{old}}} = (0.333)^{1/2} \left(\frac{65}{21} \right)^{1/2} = 1.016$$

This is satisfactory. The ratio of packing volumes is,

$$\frac{(\text{Volume packing})_{\text{new}}}{(\text{Volume packing})_{\text{old}}} = bc^2 = (0.333)(1.155)^2 = 0.445$$

The ratio of feed periods and cycle times can be obtained from Eqs. 24 and 25. With $R_q = 1$, these ratios are the same as the ratio of packing volumes. The design with 5 μm packing uses less than half as much packing, has slightly better resolution, and has the same pressure drop as the design with 10 μm packing.

This case study approach illustrates that columns can be scaled to use small-diameter particles regardless of the form of the equation that relates H to v and d_p .

Simplified Scaling Rules for Linear Systems

If we have an equation for H , we can obviously substitute it into Eq. 23 or Eq. 22 and then solve the result simultaneously with Eq. 21. Any equation for H can be used; however, the simpler the equation the simpler the result will be. We will use Eq. 19 since it gives very simple results and because it has the same form as the mass transfer correlations that will be used later. We will assume that $H_1 = H_2$ and that k and n in Eq. 19 are constant. Substituting Eq. 19 into Eq. 23 and introducing the scaling factors defined in Eq. 1, we obtain

$$\frac{R_{\text{new}}}{R_{\text{old}}} = \frac{b^{1/2} c^n}{a^{(n+1)/2} R_q^{n/2}} \quad (28)$$

It will be convenient to further massage this equation. Substituting Eq. 13 into Eq. 28 and squaring both sides, we obtain

$$\left(\frac{R_{new}}{R_{old}}\right)^2 = R_N = \frac{N_{new}}{N_{old}} = \frac{bc^{2n}}{a^{n+1}R_q^n} \quad (29)$$

All of the other terms are the same in the two designs and divide out. If $R_N = 1.0$, the two columns will have the same number of stages and from Eq. 13 the resolutions are the same. Equation 29 can be obtained directly by writing Eq. 20 for both old and new designs and then taking the ratio of these equations.

If we treat the particle diameter ratio a , the ratio of number of stages R_N , and the pressure ratio R_p as independent variables, Eqs. 21 and 29 can be solved for the length ratio b and the column diameter ratio c required. The results are

$$b = \frac{L_{new}}{L_{old}} = a^{(3n+1)/(n+1)} R_p^{n/(n+1)} R_N^{1/(n+1)} \quad (30)$$

and

$$c = \frac{D_{new}}{D_{old}} = a^{(n-1)/(2n+2)} \left(\frac{R_N}{R_p}\right)^{1/(2n+2)} R_q^{1/2} \quad (31)$$

The ratio of the volumes of packing required for the new and old designs is easily obtained:

$$\frac{(\text{Volume packing})_{new}}{(\text{Volume packing})_{old}} = bc^2 = a^{4n/(n+1)} R_N^{2/(n+1)} R_p^{(n-1)/(n+1)} R_q \quad (32)$$

When throughput of feed is constant, $R_q = 1$, Eq. 32 scales in the same way as Eqs. 24 and 25.

To consider the power of this scaling technique we can look at several simple numerical examples. Assume that we desire the same throughput, the same resolution, and the same pressure drop with the old and new designs and set $R_q = 1$, $R_N = 1$, and $R_p = 1$. What values of b and c should be used if the particle diameter in the new design is one-half that in the old design, $a = 0.5$? The result depends upon the value of the parameter n in Eq. 19. If $n = 1$ (pore diffusion controls), then Eq. 31 reduces to $c = 1$ and thus $D_{new} = D_{old}$. Equation 30 becomes $b = a^2$ and $L_{new} = L_{old}/4$. Equations 32, 24, and 25 show that the column requires one-fourth as much packing as the old design, the feed period is one-fourth as long, and the cycle period is one-fourth as long. The total amount of feed per hour is $(\text{feed/cycle})(\text{cycles/hour})$, which is the same in the two designs. Thus, the new design has the same resolution, the same pressure drop, and the same feed throughput, but requires one-fourth as much packing. Unless there are overwhelming practical reasons for not reducing the particle diameter, the column length, and the cycle time, the new design is superior. There may in fact be practical difficulties, and these are discussed later.

Consider the same example but with $n = 0.5$. Now Eq. 31 gives $D_{new} = 1.122D_{old}$, while Eq. 30 gives $L_{new} = 0.315L_{old}$. The column is shorter and fatter. The product bc^2 in Eqs. 32, 24, and 25 is 0.397. Thus less packing is required for the new design for the same feed throughput with the same resolution and the same Δp . For the example based on Figure 1 we found that $bc^2 = 0.445$. Adsorbent volume reduction is largest when pore diffusion controls, $n = 1$, but is significant in all cases. Obviously, much larger reductions are obtained for smaller values of a .

The scaling equations can be used to change the operating parameters R_p or R_N . For example, suppose that the pressure drop in the existing design is too high and we desire to divide the pressure drop by a factor of 2, $R_p = 0.5$. Equations 30 and 31 can be used to scale the column whether we change the particle diameter or keep it constant. For $n = 0.5$, $a = 1$ (no change in d_p), $R_q = 1$, and $R_N = 1$, the results are

$$c = \frac{D_{new}}{D_{old}} = 2^{1/3} = 1.2599, \quad b = \frac{L_{new}}{L_{old}} = \frac{1}{2^{1/3}} = 0.7937$$

and the volume of adsorbent increases by a factor of 1.2599. If we repeat this problem, but with $a = 0.5$ the results are

$$c = \frac{D_{new}}{D_{old}} = 2^{1/2} = 1.414, \quad b = \frac{L_{new}}{L_{old}} = 1/4$$

and the volume of adsorbent decreases by a factor of 2. Thus, the designer can to some extent tailor the column to give the desired pressure drop and separation. The resulting columns may be short and fat compared to classical designs, but there are no theoretical reasons for long narrow columns.

The scaling equations can also be used to change the resolution. Suppose we wish to double the resolution obtained in the existing design. Then from Eq. 29, $R_N = 4$. With $R_q = 1$, $R_p = 1$, $a = 1$, and $n = 0.5$, the resulting scale factors are

$$c = \frac{D_{new}}{D_{old}} = 4^{1/3} = 1.5874, \quad b = \frac{L_{new}}{L_{old}} = 4^{2/3} = 2.5198$$

and the volume of packing $bc^2 = 6.35$. This differs from the usual result of increasing the column length by a factor of four since the pressure drop has been kept constant in this calculation. If this calculation is repeated with $a = 0.5$, we obtain

$$c = \frac{D_{new}}{D_{old}} = \left(\frac{1}{2}\right)^{-0.5/3} 4^{1/3} = 1.7818, \quad b = \frac{L_{new}}{L_{old}} = \left(\frac{1}{2}\right)^{2.5/1.5} (4)^{1/1.5} = 0.7937$$

and the volume of packing $bc^2 = 2.5198$. Of course, for this large a change in resolution it would be advantageous to change the selectivity, α . These examples show some of the control the designer has by scaling the column and using smaller particles.

When building a new column, it is often fairly easy to change the height to any desired value, but the column diameter is fixed to the standard sizes that are readily available. Invariably, the predicted diameter will lie between two standard diameters. The designer can try one of these standard diameters. This makes c an independent variable in Eqs. 29 and 21. If $a = d_{p,new}/d_{p,old}$ and either R_N or R_p is chosen as the other independent variable, Eqs. 29 and 21 can be solved for b and either R_p or R_N . If this design is not satisfactory, the other standard diameter bracketing the solution can be tried.

Scaling of Systems with Nonlinear Isotherms

When concentrations are increased, most systems will eventually have nonlinear isotherms. Since it is often desirable to operate large-scale chromatography systems at high concentrations,

it is important to study the scaling of these systems. In order to keep the mathematics tractable we will restrict the study to solutes that are independent. Experimentally this can occur with mixed-adsorbent beds or when all but one solute are present at trace concentrations. Interacting nonlinear solutes also have considerable commercial importance. A preliminary equilibrium analysis indicates that these systems will also scale (Wankat, 1986b).

First, the scaling principles for a single solute with plateau formation will be studied. Since the solutes are independent, this provides the basis for analyzing multiple solutes. Plateaus will form if the feed pulse is long enough. When a plateau forms, the boundary conditions for the leading and trailing edges are the same as the boundary conditions for breakthrough and elution, respectively. Thus, existing solutions can be used. For shorter feed pulses there will be no plateau and no analytical solutions including mass transfer are available. This situation will be analyzed using a local equilibrium analysis.

Scaling principles for single-solute systems with plateau formation

When the solutes are independent, the separation of two solutes can be obtained by superposition of the results obtained for a single solute. Thus, we will consider the behavior of a single nonlinear solute, following the analysis of Wankat (1987). Consider a nonlinear system with a single solute with favorable equilibrium where a constant pattern forms at the leading edge and a proportional pattern forms at the trailing edge of an elution curve, as shown in Figure 2 (Lightfoot et al., 1962; Sherwood et al., 1975; Wankat 1986a). Constant-pattern waves do not change shape as they move down the column. This is illustrated in Figure 5. Proportional-pattern waves continually change shape as they move down the column. This is illustrated in Figure 6. Mass transfer is often modeled in a lumped parameter

form:

$$\rho_B(1 - \epsilon) \frac{\partial q}{\partial t} = -k_m a_p (C^* - C) \quad (33)$$

where C^* is the equilibrium concentration. To be specific, a generalized Langmuir isotherm,

$$q = \frac{a^* C^*}{1 + b^* C^*} \quad (34)$$

will be used.

For the constant-pattern wave the length of the mass transfer zone, which is arbitrarily chosen to go from $C = 0.05 C_F$ to $C = 0.95 C_F$, is (Wankat, 1986a)

$$L_{MTZ} = u_{sh} \rho_B (1 - \epsilon) \frac{q_F}{C_F} \left\{ \frac{-a^*}{a^* - \frac{q_F}{C_F}} \ln \left[\frac{(0.05)}{(0.95)} \right] + \ln \left[\frac{a^* - \frac{q_F}{C_F} - 0.95 b^* q_F}{a^* - \frac{q_F}{C_F} - 0.05 b^* q_F} \right] \right\} \quad (35)$$

where u_{sh} is the shock wave velocity or the velocity of the stoichiometric center of mass of the pattern:

$$u_{sh} = \frac{v}{1 + \frac{1 - \epsilon}{\epsilon} \rho_B \frac{\Delta q}{\Delta C}} \quad (36)$$

The mass transfer coefficient $k_m a_p$ can be correlated by (Sherwood et al., 1975)

$$k_m a_p = k \frac{v^{1-m}}{d_p^{1+m}} \quad (37)$$

where the constant of proportionality, k , is different for film and pore diffusion control. Combining Eqs. 35–37 we obtain

$$L_{MTZ} \propto v^m d_p^{1+m} \quad (38)$$

When $m = 1$, this corresponds to pore diffusion control, while when $m = 0.5$ this approximates film diffusion control. We assume that a^* , b^* , k , and m are constant over the ranges of v and d_p of interest.

During elution, favorable isotherms such as Eq. 34 will produce proportional-pattern waves. Unless mass transfer is slow, most of the proportional-pattern wave can be fairly accurately predicted from the diffusive wave calculated by the local equilibrium theory (Sherwood et al., 1975; Wankat, 1986a). Thus the proportional-pattern wave is controlled by equilibrium and its velocity can be estimated from

$$u(C) = \frac{v}{1 + \frac{1 - \epsilon}{\epsilon} \rho_B \frac{\partial q}{\partial C}} \quad (39)$$

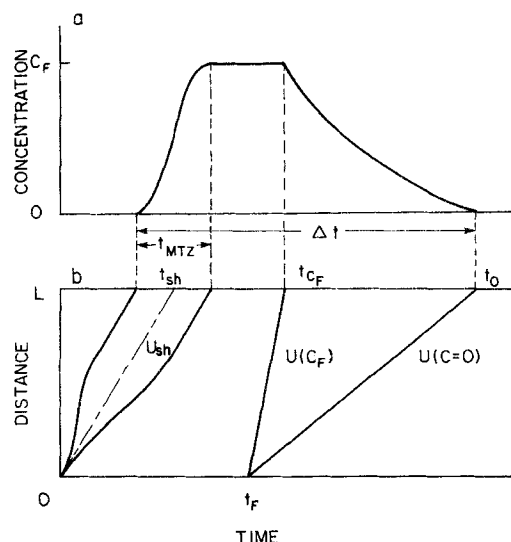


Figure 2. Constant and proportional patterns in elution for a nonlinear component.

a. Outlet concentration profile
b. Approximate paths in column

This solute velocity depends on concentration and temperature since $\partial q/\partial C$ is a function of C and T for nonlinear isotherms.

In Figure 2, the total bandwidth Δt is

$$\Delta t = t_0 - \left(t_{sh} - \frac{t_{MTZ}}{2} \right) \quad (40)$$

Since $t_0 = L/u(C=0) + t_F$ and $t_{sh} = L/u_{sh}$, this is

$$\Delta t = \frac{L}{u(C=0)} + t_F - \frac{L}{u_{sh}} + \frac{t_{MTZ}}{2} \quad (41)$$

$t_{MTZ} (= L_{MTZ}/u_{sh})$ is the time elapsed for the mass transfer zone to pass the exit of the column, and can be determined from Eqs. 36 and 38. We will take the ratio of new and old designs for each term in Eq. 41. The new design will use the scaling factors given in Eq. 1. We obtain

$$\frac{[L/u(C=0)]_{new}}{[L/u(C=0)]_{old}} = \frac{L_{new}}{L_{old}} \frac{u(C=0)_{old}}{u(C=0)_{new}} = b \frac{v_{old}}{v_{new}} = bc^2/R_q \quad (42)$$

We will use Eq. 24 to scale the feed periods. The remaining two terms in Eq. 41 are

$$\frac{(L/u_{sh})_{new}}{(L/u_{sh})_{old}} = b \frac{u_{sh,old}}{u_{sh,new}} = b \frac{v_{old}}{v_{new}} = bc^2/R_q \quad (43)$$

and

$$\frac{(t_{MTZ}/2)_{new}}{(t_{MTZ}/2)_{old}} = \frac{(L_{MTZ}/u_{sh})_{new}}{(L_{MTZ}/u_{sh})_{old}} = \frac{(v^m d_p^{1+m}/v)_{new}}{(v^m d_p^{1+m}/v)_{old}} \quad (44)$$

$$= a^{1+m} c^{2-2m} R_q^{m-1} \quad (45)$$

Every term in Eq. 41 scales as bc^2/R_q (Eqs. 42, 43, and 24) except $t_{MTZ}/2$ (Eq. 45).

After some manipulation we can express bc^2/R_q and $t_{MTZ}/2$ in terms of the variables a , R_p , R_q , and R_{MTZ} where R_{MTZ} is defined as

$$R_{MTZ} = \frac{(L/L_{MTZ})_{new}}{(L/L_{MTZ})_{old}} \quad (46)$$

The ratio L_{MTZ}/L is the fraction of the bed required for the constant-pattern portion of the wave. This ratio also controls the fractional bed use during the constant-pattern step in adsorption (Lukchis, 1973; Wankat, 1986a). If $R_{MTZ} = 1$, the old and new designs use the same fraction of the bed for the constant-pattern wave. As we will see shortly, when $R_N = 1$ and $R_{MTZ} = 1$ every part of the elution curve scales as bc^2 , and the separation between two peaks remains constant.

From Eqs. 1, 4, 38, and 46,

$$R_{MTZ} = \frac{bc^{2m}}{a^{m+1} R_q} \quad (47)$$

The scaling of the pressure drop is given by Eq. 21. Assuming that the particle diameter ratio a and the operating ratios R_{MTZ} , R_q , and R_p are independent variables, we can solve Eqs. 21 and

47 simultaneously for the required ratios of the column length and diameter:

$$b = a^{(3m+1)/(m+1)} R_p^{m/(m+1)} R_{MTZ}^{1/(m+1)} \quad (48)$$

$$c = a^{(m-1)/(2m+2)} \left(\frac{R_{MTZ}}{R_p} \right)^{1/(2m+2)} R_q^{1/2} \quad (49)$$

Thus, from Eqs. 45 and 49,

$$\frac{(t_{MTZ}/2)_{new}}{(t_{MTZ}/2)_{old}} = a^{4m/(m+1)} R_p^{(m-1)/(m+1)} R_{MTZ}^{(1-m)/(m+1)} \quad (50)$$

And from Eqs. 48 and 49,

$$bc^2/R_q = a^{4m/(m+1)} R_p^{(m-1)/(m+1)} R_{MTZ}^{2/(m+1)} \quad (51)$$

If we set $R_{MTZ} = 1$, Eqs. 50 and 51 are equal. As each part of Eq. 41 scales as bc^2/R_q , the total bandwidth scales as bc^2/R_q . Therefore, the relative position of every part of the elution peak is the same. If a separation is adequate in the old system, it will be adequate in the new system. Note that when $R_{MTZ} = R_N = 1$, Eq. 48 has the same form as Eq. 30 and Eq. 49 has the same form as Eq. 31. Thus, with the restriction that $R_{MTZ} = R_N = 1$, scaling rules for linear and nonlinear systems are identical. To keep the same throughput and separation, the feed period and cycle time should be scaled as in Eqs. 24 and 25.

Multiple-solute systems with plateaus

In chromatographic systems, several solutes are separated. We consider scaling for a nonlinear chromatographic system with two independent solutes where the feed pulse period is long enough that plateaus form. As shown in Figure 3, two-solute systems can generally be divided into three cases. The same scaling procedures as applied to the single-solute system can be used. Since the solutes are independent and there are plateaus, each portion of the wave is similar to the single-solute waves studied earlier. First, we will study the scaling of the total bandwidth and then the scaling of the separation of two adjacent elution curves. The solutes are assumed to have the same controlling mass transfer resistance so that m and n are the same.

Case I. Two Independent Nonlinear Solutes (Figure 3a). Using the same procedures as used previously, we obtain

$$\Delta t = t_{0,A_2} - \left(t_{sh,A_1} - \frac{t_{MTZ,A_1}}{2} \right) \quad (52)$$

$$= \frac{L}{u_{A_2}(C=0)} + t_F - \frac{L}{u_{sh,A_1}} + \frac{t_{MTZ,A_1}}{2} \quad (53)$$

for the bandwidth. Taking the ratios of old and new designs for each term, we obtain

$$\frac{[L/u_{A_2}(C=0)]_{new}}{[L/u_{A_2}(C=0)]_{old}} = \frac{(t_F)_{new}}{(t_F)_{old}} = \frac{(L/u_{sh,A_1})_{new}}{(L/u_{sh,A_1})_{old}} = bc^2/R_q \quad (54)$$

$$\frac{(t_{MTZ,A_1}/2)_{new}}{(t_{MTZ,A_1}/2)_{old}} = a^{4m/(m+1)} R_p^{(m-1)/(m+1)} R_{MTZ}^{(1-m)/(m+1)} \quad (55)$$

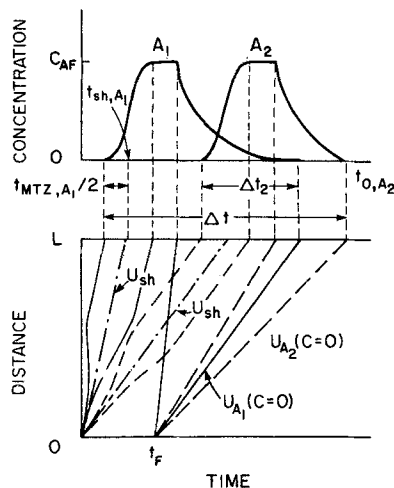


Figure 3a. Two nonlinear components.

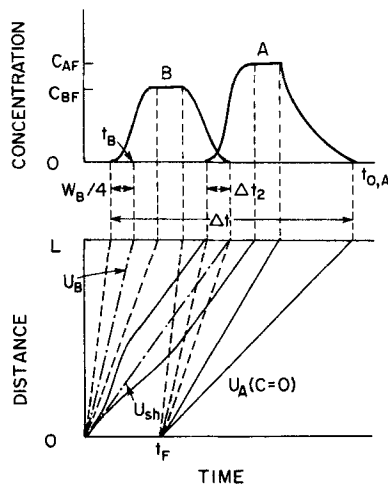


Figure 3b. One fast linear and one nonlinear component.

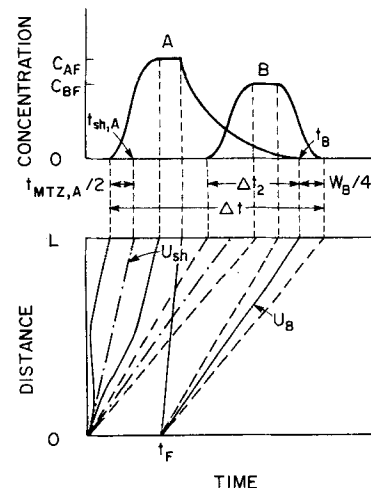


Figure 3c. One nonlinear and one slow linear component.

Figure 3. Outlet concentration profiles and approximate paths in column.

Case II. One Fast Linear Solute B Followed by One Nonlinear Solute A (Figure 3b). The bandwidth is

$$\Delta t = t_{0,A} - \left(t_B - \frac{w_B}{4} \right) \quad (56)$$

where the width w_B is given by Eq. 10. Then

$$\Delta t = \frac{L}{u_A(C=0)} + t_F - \frac{L}{u_B} + \frac{(LH_B)^{1/2}}{u_B} \quad (57)$$

Taking the ratio of old and new designs for each term, we obtain

$$\frac{[L/u_A(C=0)]_{new}}{[L/u_A(C=0)]_{old}} = \frac{(t_F)_{new}}{(t_F)_{old}} = \frac{(L/u_B)_{new}}{(L/u_B)_{old}} = bc^2/R_q \quad (58)$$

Using Eq. 19 for H , we obtain

$$\frac{[(LH_B)^{1/2}/u_B]_{new}}{[(LH_B)^{1/2}/u_B]_{old}} = b^{1/2} \frac{(v^{n/2} d_p^{(n+1)/2})_{new}}{(v^{n/2} d_p^{(n+1)/2})_{old}} \frac{v_{old}}{v_{new}} \quad (59)$$

$$= a^{(n+1)/2} b^{1/2} c^{2-n} R_q^{(n-2)/2} \quad (60)$$

Using Eqs. 30 and 31 for the scaling factors for b and c , we obtain

$$\frac{[(LH_B)^{1/2}/u_B]_{new}}{[(LH_B)^{1/2}/u_B]_{old}} = a^{4n/(n+1)} R_p^{(n-1)/(n+1)} R_N^{(3-n)/(2n+2)} \quad (61)$$

where R_N is defined by Eq. 29.

Case III. One Nonlinear Solute A Followed by One Slow Linear Solute B (Figure 3c). The bandwidth is

$$\Delta t = \left(t_B + \frac{w_B}{4} \right) - \left(t_{sh,A} - \frac{t_{MTZ,A}}{2} \right) \quad (62)$$

$$= \frac{L}{u_B} + \frac{(LH_B)^{1/2}}{u_B} + t_F - \frac{L}{u_{sh,A}} + \frac{t_{MTZ,A}}{2} \quad (63)$$

Taking the ratio of old and new designs for each term, we obtain

$$\frac{(L/u_B)_{new}}{(L/u_B)_{old}} = \frac{(t_F)_{new}}{(t_F)_{old}} = \frac{(L/u_{sh,A})_{new}}{(L/u_{sh,A})_{old}} = bc^2/R_q \quad (64)$$

$$\frac{[(LH_B)^{1/2}/u_B]_{new}}{[(LH_B)^{1/2}/u_B]_{old}} = a^{4n/(n+1)} R_p^{(n-1)/(n+1)} R_N^{(3-n)/(2n+2)} \quad (65)$$

$$\frac{(t_{MTZ}/2)_{new}}{(t_{MTZ}/2)_{old}} = a^{4m/(m+1)} R_p^{(m-1)/(m+1)} R_{MTZ}^{(1-m)/(m+1)} \quad (66)$$

If $R_N = R_{MTZ} = 1$ and $m = n$, Eqs. 55, 61, 65, and 66 are all equal. If the controlling resistance is the same for both solutes, n and m will be the same in Eqs. 19 and 37. In this case, if R_{MTZ} is set to 1 then R_N will automatically be equal to 1. Therefore, scaling rules apply successfully to the two-solute system if we require either $R_N = 1$ or $R_{MTZ} = 1$.

Scaling only the total bandwidth is not enough to assure the same separation. For the same separation, the ratio of the overlapped part of the two solutes to the total bandwidth must remain constant. It is sufficient to show that the overlapped period Δt_2 , Figure 3, scales in the same way as the total bandwidth. This will be done for each case.

Case I. For two independent nonlinear solutes the overlap is, Figure 3a:

$$\Delta t_2 = t_{0,A1} - \left(t_{sh,A2} - \frac{t_{MTZ,A2}}{2} \right) \quad (67)$$

$$= L/u_{A1}(C=0) + t_F - L/u_{sh,A2} + \frac{t_{MTZ,A2}}{2} \quad (68)$$

Equations 67 and 68 have the same forms as Eqs. 52 and 53 except that subscripts A_1 and A_2 are changed. Since the two solutes are independent of each other, the individual terms in Eq. 68 have the same forms as Eqs. 54 and 55. Then if we require $R_{MTZ} = 1$, the ratio of the new to the old overlapped periods $(\Delta t_2)_{new}/(\Delta t_2)_{old}$ becomes bc^2/R_q .

Case II. For one fast linear solute B followed by one nonlinear solute A the overlap is, Figure 3b:

$$\Delta t_2 = \left(t_B + \frac{w_B}{4} \right) - \left(t_{sh,A} - \frac{t_{MTZ,A}}{2} \right) \quad (69)$$

Since Eq. 69 has the same form as Eq. 62, $(\Delta t_2)_{new}/(\Delta t_2)_{old}$ equals bc^2/R_q if $R_{MTZ} = R_N = 1$.

Case III. For one nonlinear solute A followed by one slow linear solute B the overlap is, Figure 3c:

$$\Delta t_2 = t_{0,A} - \left(t_B - \frac{w_B}{4} \right) \quad (70)$$

Since Eq. 70 has the same form as Eq. 56, Δt_2 scales as bc^2/R_q if $R_{MTZ} = R_N = 1$.

We have shown that both the overlapped period and the total bandwidth scale as bc^2/R_q when $R_{MTZ} = R_N = 1$ and $m = n$. As a result, the ratio of the overlapped period to the total bandwidth is kept constant at different designs. Consequently, the separation is the same if the relative shapes of the curves are unchanged. Since this scaling procedure assures that each portion of the elution curve is scaled as bc^2/R_q , the relative shapes are unchanged and the separation for the old and new designs is the same.

The same procedures can be used to examine the scaling rules for systems of more than two solutes. Figure 4 shows the elution curves for two linear solutes (probably trace components) and one nonlinear solute. It can easily be shown that the three-solute systems scale in exactly the same way as the two-solute systems. Thus, we have proved that the scaling rules can be used for multiple-solute systems with mixtures of independent linear and nonlinear solutes.

To consider the power of this scaling technique we could look at numerical examples. However, when $R_{MTZ} = R_N = 1$ and $m = n$, the nonlinear and linear systems scale in the same way. Thus the results are the same as those presented earlier for linear systems.

Entrance effects

We used the constant-pattern analysis, Eq. 35, to describe the constant-pattern wave for nonlinear elution. However, this analysis applies only when the leading edge of an elution curve is fully developed. For short beds this may not be true. To examine the entrance effects, we reworked example 10.6 of Sherwood et al. (1975). A Langmuir-type isotherm was used for the adsorption equilibrium in this example. Most of the mass transfer resistance in this system is due to pore diffusion control. Elution curves following the step input were calculated by the Thomas solution (Sherwood et al., 1975; Thomas, 1944). This solution is

$$\frac{C}{C_F} = \frac{J(m/K^*, mT)}{J(m/K^*, mT) + [1 - J(m, mT/K^*)] \times \exp [(K^{*-1} - 1)m(T - 1)]} \quad (71)$$

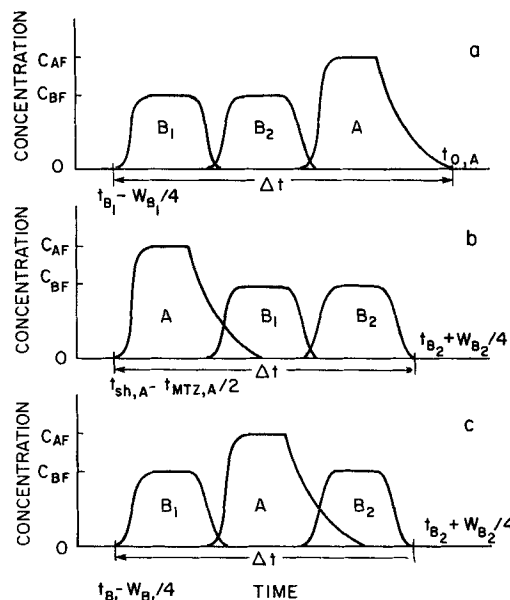


Figure 4. Elution curves for chromatographic system of two linear components and one nonlinear component.

A. Nonlinear component; B_1, B_2 , linear components
a. Two fast linear components
b. Two slow linear components
c. Fast and slow linear components

where

$$J(\alpha, \beta) = 1 - e^{-\beta} \int_0^\alpha e^{-\xi} I_0(2\sqrt{\beta\xi}) d\xi \quad (72)$$

and

$$i = \sqrt{-1} \quad (73)$$

In these equations m is dimensionless distance and mT is dimensionless time. K^* is the equilibrium constant in the Langmuir isotherm related to a^* and b^* in Eq. 16 as

$$a^* = \frac{q_m}{C_0} K^* \quad (74)$$

$$b^* = \frac{K^* - 1}{C_0} \quad (75)$$

where q_m is the capacity of the solid phase and C_0 is the total solute concentration. I_0 is the zero-order Bessel function of the first kind for a purely imaginary argument. We used the first two terms of an asymptotic series for $J(\alpha, \beta)$ since other terms are negligible with $\alpha\beta > 36$ (Sherwood et al., 1975). Then the J function simplifies to,

$$J(\alpha, \beta) = \frac{1}{2} \operatorname{erfc}(\sqrt{\alpha} - \sqrt{\beta}) + \frac{\exp [-(\sqrt{\alpha} - \sqrt{\beta})^2]}{2\pi^{1/2} [(\alpha\beta)^{1/4} + \beta^{1/2}]} \quad (76)$$

The results of the computer calculations are presented in Figure 5 and Table 1. The table shows that a longer column is needed for the constant-pattern wave to be fully developed as d_p

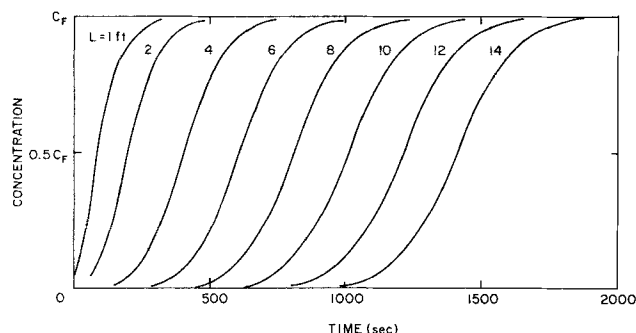


Figure 5. Constant-pattern elution curves for nonlinear component calculated by Thomas solution as a function of column length.

$d_p = 0.476$ cm

increases. It takes a column longer than 4.27 m (14 ft.) to fully develop the constant pattern for $d_p = 0.476$ cm while a 1.22 m (4 ft.) column is enough for $d_p = 0.0841$ cm.

To examine the scaling rules for short columns, calculations were done for example 10.6 of Sherwood *et al.* (1975). We calculated the wave for a given particle diameter at a specific column length. Then, the same waves were calculated for different particle diameters at column lengths the values of which were scaled from the previous column length by a^2 . Values for t_{MTZ} for each particle diameter are presented in Table 2. If the scaling rule applies with $m = 1$, $t_{MTZ}/t_{MTZ,0.476}$ should be 0.1246 $[= (0.168/0.476)^2]$ and 0.0312 $[= (0.0841/0.476)^2]$ for $d_p = 0.168$ and 0.0841 cm, respectively. The calculated results are within 3% error from the expected scaling values in most cases. Since in this example pore diffusion does not completely control, $m < 1$, a slight error is expected. Notice that the scaling rule is adequate in the range where entrance effects are important (L shorter than 3.048 m [10 ft.] and 0.6096 m [2 ft.] for $d_p = 0.168$ and 0.0841 cm, respectively, Table 1). We conclude that the scaling rules are applicable to reasonably short columns for the constant-pattern elution of a system with independent nonlinear solutes.

Proportional patterns

The mass transfer zone analysis used to describe the constant-pattern wave for nonlinear solutes includes the mass transfer

Table 1. Comparison of Constant-Pattern Elution Curves with Various Particle Diameters Calculated by Thomas Solution

Column Length m (ft.)	Particle Dia., cm		
	0.476	0.168	0.084
0.3048 (1)	233	66.9	22.5
0.6096 (2)	320	79.7	23.4
1.2192 (4)	416	88.5	23.6
1.8288 (6)	486	91.1	23.6
2.4384 (8)	532	92.0	23.6
3.048 (10)	567	92.2	23.6
3.6576 (12)	594	92.3	23.6
4.2672 (14)	616	92.3	23.6
15.24 (50)	724	92.3	23.6

Values are t_{MTZ} in s.

Table 2. Scaling Behavior of Constant-Pattern Elution Curves with Various Particle Diameters and Column Lengths Calculated by Thomas Solution

	Particle Dia., cm		
	0.476	0.168	0.084
L , m	1.524	0.190	0.0475
t_{MTZ} , s	457.1	57.39	14.55
$t_{MTZ}/t_{MTZ,0.476}$	1	0.1256	0.0318
L , m	3.048	0.3798	0.0951
t_{MTZ} , s	566.9	71.22	18.08
$t_{MTZ}/t_{MTZ,0.476}$	1	0.1256	0.0319
L , m	12.192	1.5188	3.804
t_{MTZ} , s	715.8	90.15	22.97
$t_{MTZ}/t_{MTZ,0.476}$	1	0.1259	0.0321
L , m	30.48	3.798	0.952
t_{MTZ} , s	732.5	92.33	23.56
$t_{MTZ}/t_{MTZ,0.476}$	1	0.1260	0.0322

resistance in a lumped parameter form. However, the diffusive wave analysis used to describe the proportional-pattern wave was based on local equilibrium theory and does not include the mass transfer resistance. We used the Thomas solution for the elution of an adsorbed material to examine the effect of the mass transfer resistance on the scaling. The solution for elution is (Sherwood *et al.*, 1975)

$$\frac{C}{C_F} = \frac{1 - J(m/K^*, mT)}{1 - J(m/K^*, mT) + J(m, mT/K^*) \times \exp[(K^{*-1} - 1)m(T - 1)]} \quad (77)$$

The calculated elution curves for the proportional pattern wave with $d_p = 0.476$ cm are shown in Figure 6 for the example studied previously. As expected, it takes longer for an elution curve to exit the column as the column length increases. The calculated values for scaling between $d_p = 0.476$ and 0.240 cm are presented in Table 3. The calculated results of $\Delta t/\Delta t_{0.476}$ are within 1% error from the scaling value of $a^2 = 0.2542$ $[= (0.240/0.476)^2]$. We conclude that the proportional-pattern wave of a nonlinear system will scale in essentially the same way when mass transfer resistances are included as it does for the local equilibrium theory.

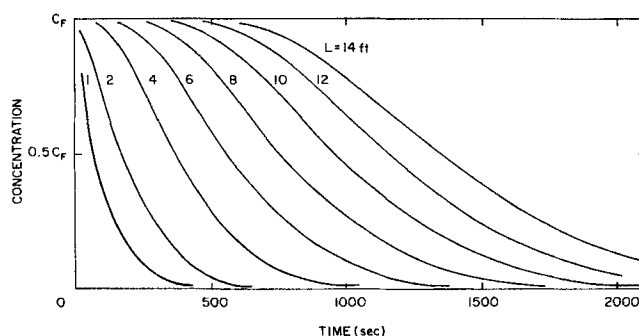


Figure 6. Proportional-pattern elution curves for nonlinear component calculated by Thomas solution as a function of column length.

$d_p = 0.476$ cm

Table 3. Scaling Behavior of Proportional-Pattern Elution Curves with Various Particle Diameters and Column Length Calculated by Thomas Solution

	Particle Dia., cm	
	0.476	0.240
L , m	1.524	0.3874
Δt , s	801.5	204.2
$\Delta t/\Delta t_{0.476}$	1	0.2548
L , m	3.048	0.7748
Δt , s	1,259	320.6
$\Delta t/\Delta t_{0.476}$	1	0.2546
L , m	6.096	1.5496
Δt , s	2,031	517.1
$\Delta t/\Delta t_{0.476}$	1	0.2546
L , m	15.24	3.874
Δt , s	4,019	1,023
$\Delta t/\Delta t_{0.476}$	1	0.2545

$$\Delta t = t(0.05 C_F) - t(0.95 C_F)$$

Multiple-solute systems without plateaus

In the previous sections we considered the scaling of nonlinear elution curves with a plateau at the feed concentration. In this section we will study the scaling of elution curves without plateaus. Neither the mass transfer zone analysis nor the Thomas solution is directly applicable since the boundary conditions are different. No analytical solutions including mass transfer are available for the nonlinear elution curve without a plateau. We will study this case with the local equilibrium theory.

Elution and breakthrough curves for a nonlinear system calculated by the local equilibrium model are shown in Figure 7 for a series of column lengths. The shock and diffusive breakthrough curves are calculated by Eqs. 36 and 39, respectively. If the column length is shorter than that equivalent to point P in Figure 7 (junction where shock and diffusive wave at the feed

concentration meet), a plateau will be present and the previous analyses are valid. The similarity between the elution curve in Figure 2 and the case of $L = 50$ cm in Figure 7 is observable except that an S-shaped constant-pattern wave develops due to mass transfer, Figure 2. Once the shock wave intersects the migration trajectory of the diffusive wave at the feed concentration (point P), the plateau at the feed concentration disappears from the elution curve. The maximum concentration of an elution curve appears as a sharp peak that decreases in height for longer columns. The velocity of the shock wave is determined by the characteristics of the adsorption isotherm (Sherwood et al., 1975; Wankat, 1986a). The shock wave in Figure 7 slows down as it travels through the column after passing junction P since the upstream concentration is continuously decreasing. The bandwidth of the elution curve is $t_0 - t_{sh}$.

The velocity of the diffusive wave at zero concentration is constant. Therefore, the paths of shock waves at different feed periods must follow the same pattern (shape) to obey the scaling rules. This can be done by setting

$$\frac{L_{new}/L_{old}}{t_{F,new}/t_{F,old}} = 1 \quad (78)$$

The results for scaling by making L/t_F constant for an actual problem are presented in Figure 8 and Table 4. The calculated results show that this scaling works for the equilibrium analysis for nonlinear elution without a plateau. The exact scaling values are 0.5 ($= 200/400$) and 0.25 ($= 100/400$) for $\Delta t_{200}/\Delta t_{400}$ and $\Delta t_{100}/\Delta t_{400}$, respectively.

Using the previous scaling procedure, Eqs. 24 and 49, we obtain

$$\frac{L_{new}/L_{old}}{t_{F,new}/t_{F,old}} = \frac{bR_q}{bc^2} = \frac{R_q}{c^2} = a^{(1-m)/(m+1)} \left(\frac{R_{MTZ}}{R_p} \right)^{-1/(m+1)} \quad (79)$$

If we desire the same separation, $R_{MTZ} = 1$, and the same pres-

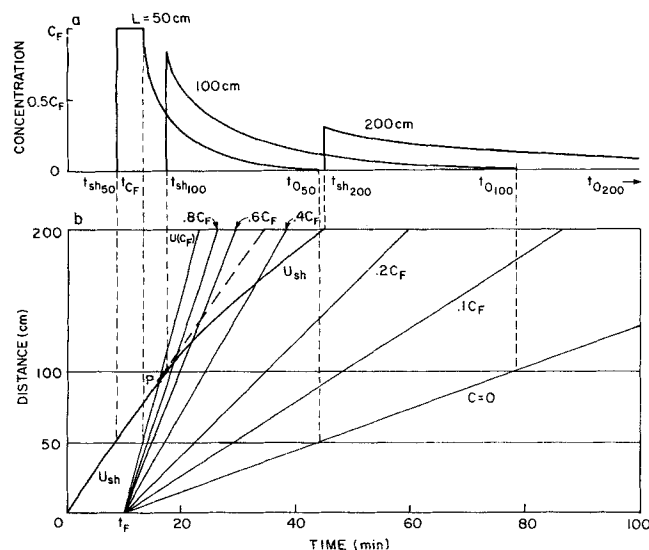


Figure 7. Shock and diffusive waves for a nonlinear component calculated by local equilibrium model.

a. Outlet concentrations
b. Characteristic solution

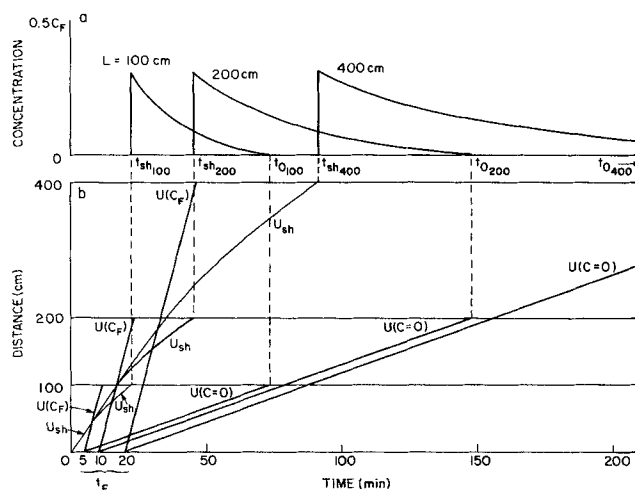


Figure 8. Scaling of shock and diffusive waves among three columns with different length and feed periods.

Calculation is by local equilibrium model
a. Outlet concentration profiles
b. Characteristic solution

Table 4. Scaling Behavior of Shock and Diffusive Waves when There Is No Plateau with Various Column Lengths Calculated by Local Equilibrium Model (Figure 8)

	Column Length, m		
	4.0	2.0	1.0
t_F , min	20	10	5
t_{sh} , min	91.09	45.42	22.74
t_{C-0} , min	295.9	147.9	74.03
Δt , min	204.8	102.5	51.29
$\Delta t/\Delta t_{400}$	1	0.5006	0.2505

sure drop, $R_p = 1$, Eq. 79 simplifies to

$$\frac{L_{new}/L_{old}}{t_{F,new}/t_{F,old}} = a^{(1-m)/(m+1)} \quad (80)$$

If pore diffusion controls, $m = 1$ and Eq. 80 becomes Eq. 78. Note that the previous scaling method gives Eq. 78 exactly only when $R_{MTZ} = 1$, $R_p = 1$, and $m = 1$. For other values of m the equilibrium analysis and the mass transfer analysis scale slightly differently. Thus, when mass transfer resistances are important and operation is without plateaus, a numerical case study approach would be safest.

It is worthwhile to look at the scaling behaviors of two-solute systems. Three possible combinations of these systems are shown in Figure 9. The same scaling procedures used in the case with a plateau were used.

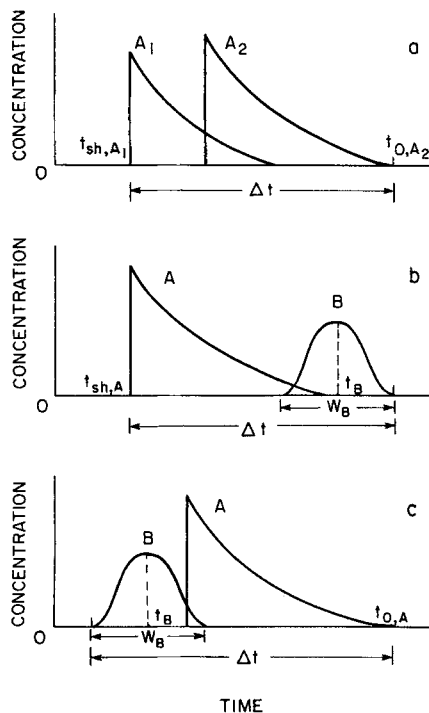


Figure 9. Elution curves of chromatographic system of linear and nonlinear components.

- A, Nonlinear components; B, linear components
a. Two nonlinear components
b. Linear (fast)-nonlinear components
c. Nonlinear-linear (slow) components

Case I. Two Nonlinear Solutes.

$$\Delta t = t_{0,A_2} - t_{sh,A_1} = \frac{L}{u_{A_2}(C=0)} - \frac{L}{u_{sh,A_1}} \quad (81)$$

Case II. One Nonlinear Solute Followed by One Slow Linear Solute.

$$\Delta t = \left(t_B + \frac{w_B}{2} \right) - t_{sh,A} = \frac{L}{u_B} + \frac{(LH_B)^{1/2}}{u_B} - \frac{L}{u_{sh,A}} \quad (82)$$

Case III. One Fast Linear Solute (Trace) Followed by One Nonlinear Solute.

$$\Delta t = t_{0,A} - \left(t_B - \frac{w_B}{2} \right) = \frac{L}{u_A(C=0)} - \frac{L}{u_B} + \frac{(LH_B)^{1/2}}{u_B} \quad (83)$$

We assume that the feed is a pulse function in these cases. As the shock wave and the diffusive wave, Figure 8 and Table 4, and linear chromatography followed the scaling rules exactly when $R_{MTZ} = R_N = R_p = n = m = 1$, two-solute systems must follow the same rules. The cases studied were:

A. Equilibrium analyses for both diffusive wave and shock wave

B. Mass transfer analysis for linear elution and equilibrium analysis for shock wave

C. Equilibrium analysis for diffusive wave and mass transfer analysis for linear elution

Following the same procedures as the case with plateau, Eqs. 67–70, we can easily show that the same separation can be achieved for the old and new designs for the two solutes without plateau when $R_N = R_{MTZ} = R_p = n = m = 1$. As a conclusion, the scaling rule applies exactly to mixtures of independent linear and nonlinear solutes without plateaus when the assumption of local equilibrium is valid and $R_N = R_{MTZ} = R_p = n = m = 1$.

The effect of mass transfer on this behavior has not yet been studied. A complete numerical analysis is required to determine the propriety of the scaling rules in nonlinear system without plateaus. However, it is very likely that the nonlinear system without plateaus with mass transfer will at least approximately follow the same scaling rules. This can be deduced from the following facts:

1. The scaling of a nonlinear system without plateaus was confirmed by the local equilibrium model when $R_p = R_N = R_{MTZ} = n = m = 1$

2. The constant-pattern and proportional-pattern waves for nonlinear systems with plateaus were verified to follow the scaling rules by the Thomas solution, which includes the mass transfer effect

3. The systems with and without plateaus are essentially the same system except that a longer column is used in the latter case

Practical Considerations

There are a variety of practical considerations that may make these scaling methods either impractical or inoperative. For various reasons to be discussed shortly there are limits on the particle sizes that can be used and still have the scaling laws be applicable. These limits are probably significant where the current (old) design uses packings in the 5 to 10 μm range. For

larger diameter packing the scaling rules are probably useful. One basic assumption of this scaling procedure is that the packing can be reused a very large number of times. If packing reuse is very limited, these methods will probably be less useful. However, they may still be of some use, since there may be less fouling of the packing per cycle because the residence time of the sample in the column is shorter.

We have assumed that the chemistry of the system is unchanged as the particle diameter is reduced. This may not be true because large particles are often easier to handle. The designer needs to find a supplier who can reliably produce the sorbent in the desired particle size. Within the range of larger packings often used for preparative separations there may be little or no change in cost as d_p decreases until quite small diameters are used. For example, Sephadex G-25 coarse, medium, and fine all cost exactly the same per kilogram, while superfine costs 41% more (Pharmacia, 1986). In this case there will be no cost penalty in designing a size exclusion chromatography system using fine instead of coarse, and much less packing can be used. The use of superfine will probably be economic even though the packing is more expensive per kilogram.

Obviously, packing the column properly with smaller diameter packing is critical to achieve the full advantage of the smaller diameter packings. Methods for doing this have been developed (Bidlingmeyer, 1987). It should be noted that a packing technique that is satisfactory with a large-diameter packing may not be successful with a smaller diameter packing. Careful sieving of the packing material is important and may be more difficult with smaller particles. The most important consideration seems to be avoiding the presence of fines. The problem of obtaining very sharp particle size distributions with small particles appears to have been solved (at a price) with monosize particles.

Equipment design becomes more critical as the column and feed pulse size decrease. Extracolumn effects (spreading of the zone in distributors, tubes, valves, tees, etc.) have been ignored in the analysis presented here. Extracolumn effects are potentially more important in short columns using small-diameter particles (Dolan, 1986). Thus connectors, valves, and distributors must be designed to minimize dead volumes. As d_p is reduced, the reduction of dead volumes in large-scale systems will probably limit the usefulness of further reduction in d_p . However, many commercial systems are well above these limits and considerable reductions in size can be obtained.

The scaling laws for nonlinear systems were derived to keep the resolution constant for the old and new designs. However, the time between peaks is reduced for columns using smaller particles. Thus timing of valves becomes more critical, and errors in timing or measurement lags become more important. Ultimately, the accuracy and speed of opening and closing valves puts a limit on faster cycling.

As the velocity and particle size change, the controlling resistance may change. This means that Eqs. 19 and 37 may be valid over fairly restricted ranges of v and d_p . Thus the scaling rules that result from Eqs. 19 and 37 may be only qualitatively correct. The values of n and m in Eqs. 19 and 37 are very important, but unfortunately may be difficult to determine accurately, particularly over limited ranges of velocity. When pore diffusion controls, $m = n = 1$, and no change in column diameter is required if $R_q = R_N = R_{MTZ} = R_p = 1$, whereas for $m = n = 0.5$ an increase in column diameter is required. A safety factor can be built into the design by designing for a higher resolution or a

higher feed throughput than is really necessary. Then if the effective values of m or n are lower than expected the operating conditions can be adjusted. An alternate design procedure is to use a case study method based on experimental data, and not rely on Eqs. 19 and 37.

Discussion

Obviously, the scaling equations developed here depend upon the form of the pressure drop and mass transfer coefficient correlations. Wankat (1987) showed that alternate scaling rules for adsorption systems are easily developed for turbulent flow. Scaling for chromatography systems with turbulent flow probably follows scaling rules similar to those for adsorption. Knox and Pyper (1986) used a different approach to study the optimization of large-scale chromatography. They found that L/d_p^2 was the controlling parameter.

Causes of zone spreading other than mass transfer, such as molecular diffusion, eddy diffusion, and extra column zone spreading, will eventually become important as the particle diameter is decreased. Thus, Eqs. 19 and 37 will eventually not be valid, and the resulting scaling equations derived here will not be valid. However, the basic idea behind this scaling remains valid. This basic idea is to reduce the particle diameter and then find a new column length and diameter, and a new feed period and cycle time that will make separation, pressure drop, and total feed throughput the same. The result will be a shorter column using less packing. If experimental data relating $k_m a_p$ and H to v and d_p are available, a case study approach can be used to find the new column dimensions and cycle times.

As the particles become smaller and the bed becomes shorter it looks less and less like a typical packed bed. Since packing the bed properly becomes absolutely critical, an obvious step is to look for alternatives to discrete particles. Microporous slabs or membranes or consolidated particles could be used. There would now be bulk flow through the pores. This step is roughly analogous to switching from dumped to structured packings in distillation. At least one such material is commercially available (Kontes, 1988). This is a microporous PVC block that has silica attached inside the pore, and is used for ion exchange chromatography. Other microporous materials can probably be adapted to chromatography or adsorption.

Conclusions

The scaling methods developed in this paper show that scaling rules are effective for elution chromatography with linear isotherms. They also work for nonlinear systems with plateaus when the same separation is required for the old and new designs ($R_{MTZ} = 1$). When pore diffusion controls ($n = m = 1.0$) the result simplifies and each part of the cycle scales as a^2 . Scaling for multiple-solute systems consisting of linear and nonlinear solutes follows the same procedures used for the single-solute system. The Thomas solution was used to verify the scaling rules for the entrance region of the constant-pattern waves and to include mass transfer for proportional-pattern waves. The scaling of nonlinear systems without plateaus was examined with the local equilibrium model. The scaling obeys the same rules when $R_N = R_{MTZ} = R_p = m = n = 1$. With these scaling rules the new design can achieve the same separation with the same pressure drop with the same throughput of feed but in a significantly shorter column.

Acknowledgment

Discussions with Donna Nugent, Sung-Sup Suh, and Nar-simhan Sundaram were helpful. This research was partially supported by National Science Foundation Grant Nos. CBT-8520700 and EET-8613167.

Notation

$a = d_{p, \text{new}}/d_{p, \text{old}}$, ratio of particle diameters in two designs
 a_p = area/volume ratio of packing, m^{-1}
 A = eddy diffusion term in Van Deemter eq., m
 A_c = cross-sectional area, m^2
 $b = L_{\text{new}}/L_{\text{old}}$, ratio of column lengths in two designs
 a^*, b^* = constants in Langmuir isotherm, Eq. 34
 B = molecular diffusion term in Van Deemter eq., s^{-1}
 c_M, c_{SM} = constants, Eq. 18
 C = mass transfer term in Van Deemter eq., s; concentration, mol/m^3
 C^* = concentration at equilibrium, mol/m^3
 C_F = feed concentration, mol/m^3
 C_0 = total solute concentration, mol/m^3
 C_M, C_{SM} = mass transfer terms in Van Deemter eq., s
 d_p = particle diameter, m
 D = column diameter, m
 D_M, D_{SM} = molecular diffusivity in fluid and stationary phase, m^2/s
 H = height equivalent to a theoretical plate, m
 I_0 = zero-order Bessel function
 J = Thomas function, Eqs. 72, 76
 k = constant, Eqs. 19, 37
 k' = capacity factor, Eq. 7
 \bar{k}' = average capacity factor, Eq. 14
 k_m = mass transfer coefficient, m/s
 K = linear equilibrium constant, $q = KC$; permeability, Eq. 3
 K^* = Langmuir equilibrium constant, Eq. 74
 L = column length, m
 L_{MTZ} = length of mass transfer zone, m
 m = dimensionless distance in Thomas solution, Eqs. 71, 77; exponent, Eq. 37
 n = exponent, Eq. 19
 N = number of stages
 Δp = pressure drop, psi
 q = amount adsorbed, mol/kg
 $q_F = q$ in equilibrium with C_F , mol/kg
 q_m = capacity of solid phase, mol/kg
 Q = volumetric flow rate, m^3/s
 R = resolution, Eq. 9
 R_{MTZ} = ratio of L/L_{MTZ} for old and new designs for nonlinear systems
 $R_N = N_{\text{new}}/N_{\text{old}}$, ratio of number of stages for linear systems
 $R_p = \Delta p_{\text{new}}/\Delta p_{\text{old}}$, ratio of pressure drops
 $R_q = Q_{\text{new}}/Q_{\text{old}}$, ratio of volumetric flow rates
 t = time, s
 t_B = time for linear wave, s
 t_F = feed time, s
 t_{MTZ} = time for mass transfer zone, s
 $t_{R,i}$ = retention time of species i , s
 t_0 = time for diffusive wave at zero concentration, s
 T = dimensionless time in Thomas solution, Eqs. 71, 77
 u_i = velocity of linear solute wave, m/s
 $u(C)$ = velocity of diffusive wave, m/s
 u_{sh} = velocity of shock wave, m/s
 $u(C_F)$ = velocity of diffusive wave at feed concentration, m/s
 $u(C=0)$ = velocity of diffusive wave at zero concentration, m/s
 v = interstitial velocity, m/s
 v_0 = superficial velocity, m/s
 w_B = width of linear peak, m

Greek letters

α = selectivity, Eq. 14
 ΔC = change in C across shock wave, mol/m^3

Δq = change in q across shock wave, mol/kg
 Δt = time for bandwidth, s
 Δt_2 = time for overlapped period of two peaks, s
 $\Delta t_{0.476}$ = time for bandwidth at $d_p = 0.476$ cm, s
 ϵ = porosity
 μ = viscosity, kg/ms
 λ = constant, Eq. 16
 γ = tortuosity, Eq. 17
 $\sigma_{i,i}$ = standard deviation in Gaussian peak, Eq. 10, s
 ρ_B = bulk density, kg/m^3

Literature Cited

- Bidlingmeyer, B. A., *Preparative Liquid Chromatography*, Elsevier, New York (1987).
 Bird, R. B., W. E. Stewart, and E. N. Lightfoot, *Transport Phenomena*, Wiley, New York (1960).
 Dolan, J. W., "Extracolumn Effects: Two Case Studies," *LC-GC*, **4**, 1086 (1986).
 Dong, M. W., and J. R. Gant, "Short Three-Micron Columns," *LC, Liq. Chromatogr. HPLC Mag.*, **2**, 294 (1984).
 Grushka, E., L. R. Snyder, and J. H. Knox, "Advances in Band Spreading Theories," *J. Chromatogr. Sci.*, **13**, 25 (1975).
 Guiochon, G., and H. Colin, "Theoretical Concepts and Optimization in Preparative-Scale Liquid Chromatography," *Chromatogr. Forum*, **1**(3), 21 (1986).
 Knox, J. H., and H. M. Pyper, "Framework for Maximizing Throughput in Preparative Liquid Chromatography," *J. Chromatogr.*, **363**, 1 (1986).
 Kontes Life Science Products, *Kontes Fastchrom Microporous Media Chromatography*, Catalog LS-88, Kontes, Vineland, NJ (Jan., 1988).
 Ladisch, M. R., M. Voloch, and B. J. Jacobson, "Bioseparations: Column Design Factors in Liquid Chromatography," *Biotechnol. Bioeng. Symp.*, No. 14, 525 (1984).
 Lightfoot, E. N., R. J. Sanchez-Palma, and D. O. Edwards, "Chromatography and Allied Fixed-Bed Separation Processes," *New Chemical Engineering Separation Techniques*, H. M. Schoen, ed., Interscience, New York, 99 (1962).
 Lukchis, G. M., "Adsorption Systems. I: Design by Mass Transfer Zone Concept," *Chem. Eng.*, **80**(13), 111 (1973).
 Majors, R. E., "Practical Aspects of Preparative Liquid Chromatography," *LC, Liq. Chromatogr. HPLC Mag.*, **3**, 862 (1985).
 Pharmacia Inc., *Pharmacia Biotechnology Products Price List 86*, Pharmacia Inc., Piscataway, NJ (1986).
 Pieri, G., P. Piccardi, G. Muratori, and L. Caval, "Scale-up for Preparative Liquid Chromatography of Fine Chemicals," *La Chimica E. L'Industria*, **65**, 331 (1983).
 Sherwood, T. K., R. L. Pigford, and C. R. Wilke, *Mass Transfer*, McGraw-Hill, New York (1975).
 Snyder, L. R., "A Rapid Approach to Selecting the Best Experimental Conditions for High-Speed Liquid Column Chromatography. II: Estimating Column Length, Operating Pressure, and Separation Time for Some Required Sample Resolution," *J. Chromatogr. Sci.*, **10**, 369 (1972).
 Thomas, H. C., "Heterogeneous Ion Exchange in a Flowing System," *J. Am. Chem. Soc.*, **66**, 1664 (1944).
 Van Deemter, J. J., F. J. Zuiderweg, and A. Klinkenberg, "Longitudinal Diffusion and Resistance to Mass Transfer as Causes of Nonideality in Chromatography," *Chem. Eng. Sci.*, **5**, 271 (1956).
 Verzele, M., and C. Dewaele, "Preparative Liquid Chromatography—A Critical Review: 1980–1984," *LC, Liq. Chromatogr. HPLC Mag.*, **3**(1), 22 (1985).
 Wankat, P. C., *Large-Scale Adsorption and Chromatography*, CRC Press, Boca Raton, FL (1986a).
 ———, "Efficient Fractionation by Ion Exchange," *Ion Exchange: Science and Technology*, A. E. Rodrigues, ed., Nijhoff, Dordrecht, Netherlands, 337 (1986b).
 ———, "Intensification of Sorption Process," *Ind. Eng. Chem. Res.*, **26**, 1579 (1987).

Manuscript received July 29, 1987, and revision received Feb. 9, 1988.